Original Article

Analysis of Sutural Strain in Maxillary Protraction Therapy

Christof Holberg[a]; Luai Mahaini[b]; Ingrid Rudzki[c]

ABSTRACT

Objective: The goal of the study was to examine the strain in the sutures of the midface and the cranial base with maxillary protraction therapy and to clarify whether such stretching suggests a skeletal effect of the apparatus employed for that purpose.

Materials and Methods: Using a finite elements model, a maxillary protraction therapy was simulated with various force levels and vectors, and the strains appearing at the sutures (in μstrain) were measured at the midface and the cranial base. The simulation model we employed consisted of 53,555 individual elements; the simulated forces were 2 × 3 N and 2 × 5 N, while the vectors of the applied forces were in the anterior and anterior caudal direction.

Results: The maximum measured strains were on average below 10 μstrain, while higher values were measured only at the nasal bone and at the cranial base at the oval and spinous foramina with anterior directed force vectors (26.4 μstrain). With an anterior-caudal force vector, the measured values were usually lower.

Discussion: The measured strains were on average about hundredfold lower than the Frost thresholds (2000 μstrain). It does not seem probable that the strains occurring upon maxillary protraction therapy suffice to stimulate any additional bone growth.

Conclusion: The good clinical efficacy of maxillary protraction therapy is apparently based, for the most part, on dental effects, while its skeletal effects still remain doubtful.

KEY WORDS: Maxillary protraction; Face mask; Finite element method; Sutural strain

INTRODUCTION

Maxillary protraction therapy using a facial mask[1,2] is a well-proven procedure employed in prepubertal Class III therapy.[3,4] By applying an anteriorly directed, orthopedic force vector to the superior dental arch, growth of the maxilla should be encouraged in an anterior direction,[5] whereby force vectors are applied to the maxillary structures by using various facial masks such as those developed by Delaire[6] or Grummons[7] or by using reverse-pull headgear.[8] As a result of the anterior directed force vectors reproaching on the dental arch, a mesial movement of the posterior teeth and a protrusion of the anterior upper jaw teeth occurs,[4,9] which facilitates a dental compensation of the skeletal dysgnathia for Class III cases.

The skeletal effects of maxillary protraction therapy, however, are still largely unclear and the subject of some controversy in the literature, although there is agreement that a slight increase in both the SNA and the ANB occurs during maxillary protraction therapy.[4,10] This clearly does not prove a skeletal effect of the apparatus, however, since no differentiation was made between growth and apparatus effects in most of the papers published. Sung and Baik,[11] on the other hand, confirmed that when comparing a protraction group with a control group of the same age showing normal growth, no significant difference could be found between the groups.

Disagreement also prevails regarding the influence of patient age on the skeletal effectiveness of the protraction therapy. In a meta-analysis, Kim et al[12] showed that the younger the patient, the larger the therapeutic effect of protraction therapy, while Cha et

[a] Postdoctoral, Department of Orthodontics, University of Munich, Munich, Germany.

[b] Resident, Department of Orthodontics, University of Munich, Munich, Germany.

[c] Professor and Department Head, Department of Orthodontics, University of Munich, Munich, Germany.

Corresponding author: Christof Holberg, MD, DDS, Department of Orthodontics, University of Munich, Goethestrasse 70, 80336 Munich, Germany
(e-mail: christof.holberg@kfo.med.uni-muenchen.de)

Accepted: February 2006. Submitted: September 2005.

 DOI: 10.2319/090505-312

Table 1. Parameters and Conditions of Simulation Model

Parameter	Conditions in the Study
Young's modulus skull	12.0 GPa
Young's modulus teeth	22.0 GPa
Poisson's ratio	0.3
Parts of each model	1 skull, 14 teeth
Number of elements	53,555
Number of nodes	97,550
Zero-displacement	Nodes at the edge of foramen magnum
Maxillary protraction	Force at nodes of the palatal side of upper jaw in the region of the canines
Level of force	2 × 3 N, 2 × 5 N

al[13] showed this effect strongly decreases after puberty. According to Merwin et al,[14] no significant differences could be shown in the therapeutic effect between the age groups of 5–8 years and 8–12 years. The skeletal effect of the maxillary protraction therapy, therefore, has not been proven in the studies published until now.

Also, the idea that a skeletal effect results from straining of the facial and cranial sutures with subsequent stimulation of the proliferative cells in the sutures[15] is of a purely hypothetical nature, since the size and vector of the strain occurring in the sutures during a maxillary protraction therapy has not yet been determined. The aim of the present paper was, therefore, to analyze the strain (in μstrain) occurring during maxillary protraction therapy in the individual sutures using an idealized finite element model of the facial skull and the cranial base.

MATERIALS AND METHODS

For carrying out the calculations and virtual experiments, an idealized simulation model (finite elements method) of the human facial skull and cranial base was employed. The model consisted of 53,555 tetrahedral, parametric single elements and 97,550 nodes (Table 1 and Figure 1). The topology of element SOLID 187 was tetrahydral with 4 nodes at each corner, 6 lines between the corners and 6 nodes which halved each line, so each tetrahydral element consisted of 10 nodes. SOLID 187 had a quadratic displacement be-

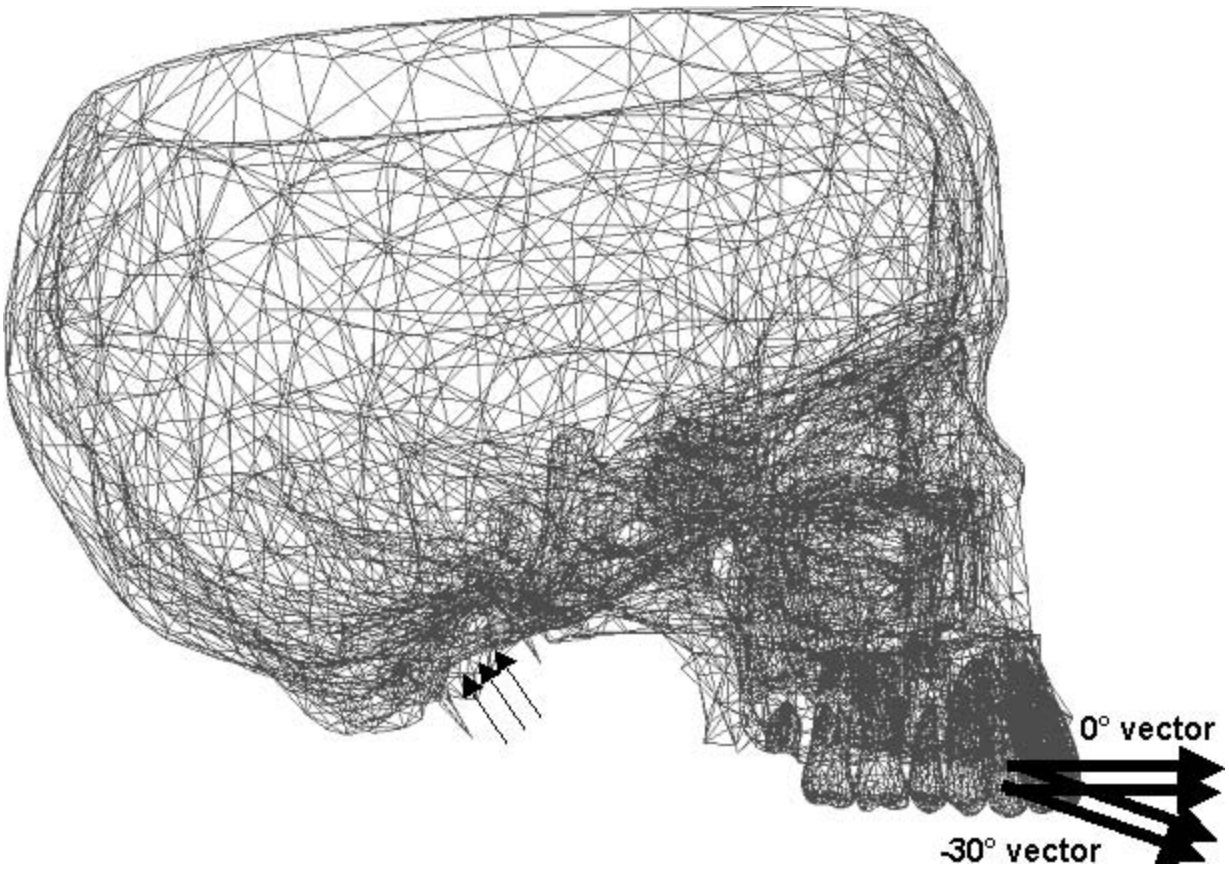

Figure 1. Finite element model with 53,555 individual elements and 97,550 nodes that was anchored in the area of the greater foramen (small arrows). In the palatinal area of the upper jaw canines, two force vectors were applied, which during the first series of experiments were directed towards anterior (0° to the occlusion plane) and during the second series of experiments towards anterior caudal (−30° to the occlusion plane).

havior and was well suited to modeling irregular meshes.

The geometric data from the individual model components were acquired using a three-dimensional scanner (Minolta, Langenhagen, Germany), an anatomic plastic model of the skull (Somso, Coburg, Germany), and a new procedure for converting numeric raw data records into analytical geometric representations.[16] The anatomic plastic model was a precise copy of a 25-year-old male skull. As the cavity of each maxillary sinus was constructed virtually, the cavities of other sinuses were ignored. The anatomic plastic model was used as the geometric basis because this model represented an average anatomic situation.

The idealized mathematical model produced this way was assigned linear properties so that modulus of elasticity results were 12 GPa for the skeletal parts and 22 GPa for the dental parts. The Poisson's ratio lay at 0.3. All teeth of the upper dental arch got the interdental contact condition ''fixed'', so they were joined together to simulate the situation including a rigid and fixed appliance attached to all teeth. The simulation model was to be fixed at several nodes in the area of the greater foramen, and a force was to be applied to the maxilla in each case on the palatal side of the crown of the upper canines. In the first series two forces of 3 N and in the second series two forces of 5 N were applied (Table 1). The direction of the force vectors was first straight and parallel to the occlusion plane in the anterior direction and, in a further series of experiments, in the anterior and caudal directions at an angle of −30° to the occlusion plane (Figure 1).

In the mathematical model it was assumed that there was no mobility in the sutures, so that the strain values were determined only by the material and geometric properties of the skull. After setting the boundary conditions and applying the corresponding force vectors, four different simulations were carried out (Table 2, von Mises Strain), whereby the vector directions of 0° and 30° were combined in each case with 2 × 3 N and 2 × 5 N. The maximum and minimum strains (in μstrain) could be recorded at the facial and cranial sutures and at the anatomic structures of the midface and the cranial base using an interactive measurement tool. All calculations and measurements were carried out using the Design Space® software (ANSYS Inc, Southpointe, Canonsburg, Pa). All measured strains (in μstrain) were recorded in tabular form and the relationships between the values were visualized using histograms (Figures 4–7).

RESULTS

At a force of 5 N (vector 0°) the minimum strain at the lacrimomaxillary suture was 2.8 μstrain, while the maximum was 18.9 μstrain (Table 2, Figure 3). On the other hand, there were also anatomic structures for which the measured variations were much smaller. Thus, at a force of 5 N (vector 0°) the minimum strain at the spheno-occipital synchondrosis was 3.1 μstrain and the maximum was 4.8 μstrain (Table 2). The differences in the maximum strains after application of 3 N and 5 N were sometimes considerable. At the lacrimomaxillary suture with 3 N (vector 0°) the maximum strain was 4.6 μstrain, while with 5 N (vector 0°) it was 18.9 μstrain (Table 2, Figures 2 and 3).

Force Vector Directed Anteriorly (Vector 0°)

High peak values were measured at the following sutures: nasomaxillary, nasofrontal, frontomaxillary, sphenotemporal, sphenofrontal, and the pterygomaxillary junction (Table 2, Figures 4–7). At the remaining measurement points in the midface, the strains at an applied strength of 3 N lay at most between 0.6 μstrain (infraorbital margin) and 13.4 μstrain (pterygoid fossa), while with a strength of 5 N they lay between 3.4 μstrain (zygomaticoalveolar crest) and 14.6 μstrain (lateral lamina of pterygoid process). The highest peak values were always measured in the area of the pterygoid processes (Table 2, Figures 4–7). At the cranial base the maximally measured strains at 3 N were between 4.0 μstrain (round foramen) and 10.4 μstrain (optic foramen), while at 5 N they were between 7.7 μstrain (round foramen) and 24.2 μstrain (oval foramen). Relatively high peak values were seen at the optic foramen, the superior orbital fissure, the spinous foramen, and the oval foramen (Table 2, Figures 4–7).

Force Vector Directed Anterior-Caudally (Vector −30°)

With an applied strength of 3 N, the maximal strains measured in the sutures lay between 0.7 μstrain (zygomaticotemporal suture) and 7.3 μstrain (spheno-occipital synchondrosis), while at 5 N they lay between 0.8 μstrain (frontoparietal suture) and 11.2 μstrain (pterygomaxillary junction). Particularly high peak values were measured at the sphenotemporal suture, the sphenofrontal suture, the spheno-occipital suture, and the pterygomaxillary junction (Table 2, Figures 4–7).

At the remaining measurement points in the midface, the strains at an applied force of 3 N lay maximally between 0.4 μstrain (in the infraorbital margin) and 7.6 μstrain (medial and lateral lamina of the pterygoid process), while at a force of 5 N they lay between 0.9 μstrain (in the infraorbital margin) and 12.9 μstrain (lateral lamina of pterygoid process). The highest peak values were always measured in the area of the pterygoid processes (Table 2, Figures 4–7). At the

Table 2. Strains of Four Different Simulations at Two Different Levels of Force

	von Mises Strain (in μstrain)							
	2 × 3 N				2 × 5 N			
	Vector 0°		Vector −30°		Vector 0°		Vector −30°	
Anatomic Structure	Min	Max	Min	Max	Min	Max	Min	Max
Sutures								
Zygomaticomaxillary suture	0.2	1.7	0.1	0.9	0.7	3.5	0.2	1.9
Zygomaticotemporal suture	0.6	1.2	0.3	0.7	0.6	7.8	0.6	2.2
Zygomaticofrontal suture	1.0	3.2	0.8	1.8	1.7	3.3	2.1	3.3
Nasomaxillary suture	0.4	2.7	0.2	1.4	9.6	26.4	0.5	2.7
Nasofrontal suture	0.7	1.9	0.3	1.2	9.3	11.4	0.7	1.8
Frontomaxillary suture	0.6	3.1	0.3	1.8	7.5	15.3	0.6	3.3
Lacrimomaxillary suture	0.4	4.6	0.3	2.8	2.8	18.9	0.5	3.8
Lacrimofrontal suture	1.2	1.9	0.9	1.7	6.3	8.2	0.8	1.6
Frontoparietal suture	0.0	0.9	0.0	0.4	0.2	3.1	0.0	0.8
Sphenotemporal	2.2	7.8	1.7	4.1	3.8	11.4	2.6	10.2
Sphenofrontal suture	2.4	8.9	1.8	5.2	2.7	5.2	1.7	6.2
Parietotemporal suture	0.0	0.6	0.0	0.8	0.8	3.4	0.2	1.8
Parieto-occipital suture	0.2	1.0	0.3	1.7	0.3	2.7	0.7	1.7
Occipitotemporal suture	0.6	3.1	0.4	1.9	0.6	3.7	1.2	3.9
Spheno-occipital synchondrosis	2.1	6.8	1.8	7.3	3.1	4.8	4.1	8.7
Pterygomaxillary junction	0.4	2.6	0.2	6.1	0.7	12.8	0.3	11.2
Midface								
Zygomaticoalveolar crest	0.7	1.9	0.2	1.1	1.8	3.4	0.7	2.8
Infraorbital margin	0.4	0.6	0.2	0.4	3.2	4.1	0.3	0.9
Anterior wall of maxillary sinus	0.3	2.5	0.1	0.7	0.8	6.4	0.2	1.8
Supraorbital margin	1.1	2.0	0.5	1.1	1.9	8.2	0.9	1.7
Medial lamina of pterygoid	0.2	10.7	0.8	7.6	0.1	8.9	0.2	11.6
Pterygoid fossa	7.7	13.4	4.2	7.4	7.2	12.4	0.8	11.2
Lateral lamina of pterygoid	0.2	9.1	0.3	7.6	0.8	14.6	0.6	12.9
Cranial base								
Optic formen	5.9	10.4	1.4	6.9	0.1	8.1	2.4	10.9
Superior orbital fissure	2.0	5.8	1.3	4.8	4.6	11.9	2.1	8.0
Spinous foramen	4.0	8.8	2.7	6.5	6.3	23.1	2.7	11.7
Oval foramen	2.7	9.4	1.8	4.3	5.7	24.2	3.3	16.4
Lacerated foramen	1.9	5.5	0.6	4.1	1.3	7.9	1.9	7.5
Round foramen	1.8	4.0	1.0	2.7	2.2	7.7	2.3	4.9

cranial base, the maximally measured strains at 3 N were between 2.7 μstrain (round foramen) and 6.9 μstrain (optic foramen), while at 5 N they lay between 4.9 μstrain (round foramen) and 16.4 μstrain (oval foramen). Relatively high peak values were measured at the optic foramen, the superior orbital fissure, the spinous foramen, and the oval foramen (Table 2, Figures 4–7).

DISCUSSION

Finite element method (FEM) is a helpful mathematical instrument for use in orthodontics.[17–21] The simulation models applied here represent an idealization of reality. The more refined FEM models are, the more precise and realistic the simulation results. The anatomic precision of the simulation models has improved greatly over the last years. In 1994 Miyasaka-Hiraga et al[22] had an FEM model of the skull that consisted of 1776 individual elements that was somewhat refined by Iseri et al[17] in 1998 to include 2349 individual elements. An FEM model of a dog's skull with 3007 elements was created by Verrue et al[23] in 2001. The geometric precision was improved further by Jafari et al[18] in 2003 so that a simulation model of the skull with 6951 elements was created.

Compared to the formerly available FEM models of the skull, the degree of anatomic differentiation was further improved in this study, so that even finer anatomic structures (eg, the foramina of the cranial base) could be considered in the mathematical model. The overall model of the facial skull and the cranial base consisted of more than 50,000 individual elements with almost 100,000 nodes. The chosen Young's modulus for the compact bone of the skull was some smaller than published by Tanne et al,[24,25] because maxillary protraction is not only used in juveniles, but also

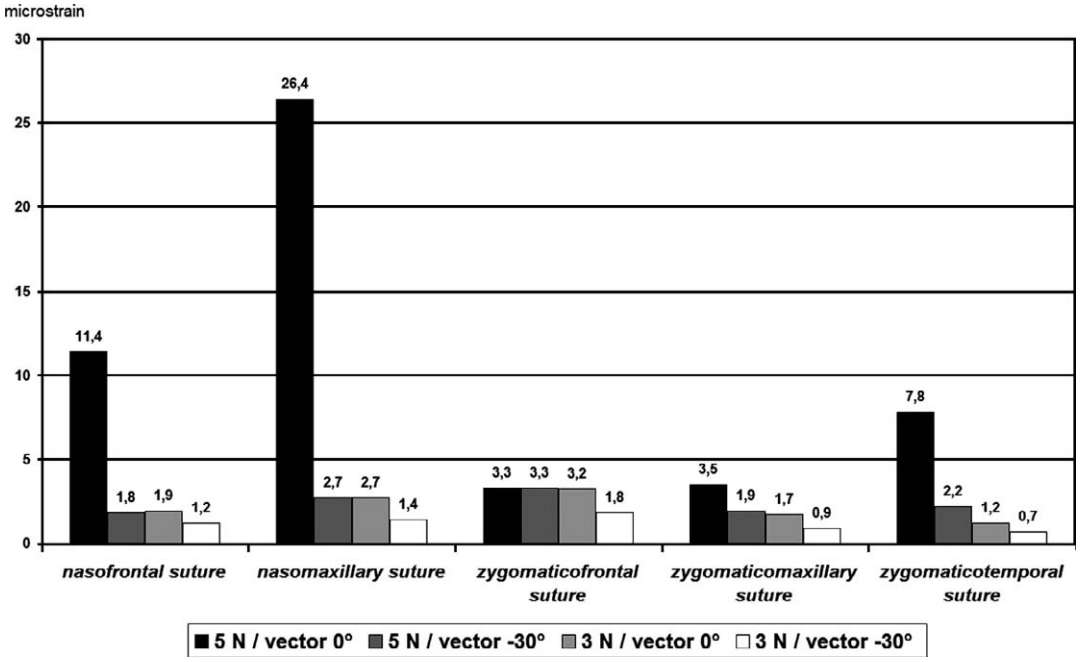

Figure 4. Strain values measured at the sutures of the midface with horizontal pulling at 5 N and at 3 N in the anterior (vector 0°) and in the anterior caudal (vector −30°) direction.

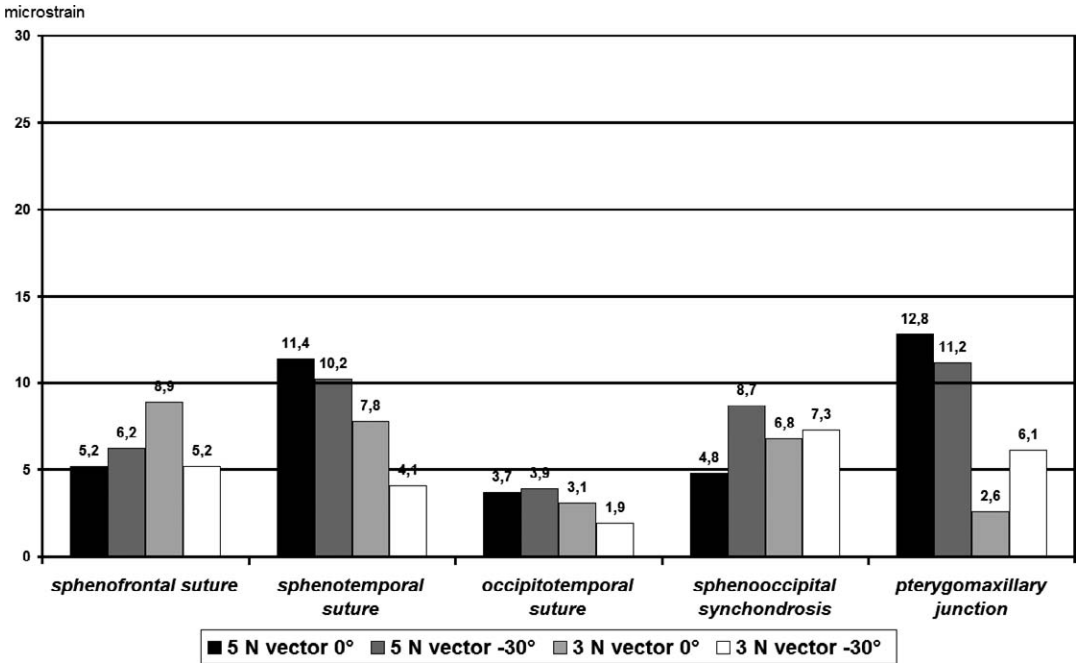

Figure 5. Strain values at the sutures of the cranial base with horizontal pulling at 5 N and at 3 N in the anterior (vector 0°) and in the anterior caudal (vector −30°) direction.

used in 6- to 8-year-old children who have bony structures with higher elasticity. Despite the relatively refined depiction of the complex skull geometry, the current results allow only statements of principle to be made about the distribution of strains with Delaire therapy, since it is an assembled simulation model with predefined properties based on averaged values.[22,24,25]

The geometric basis for the simulation model was a precise copy of a 25-year-old male skull with an average anatomic situation, but because of the scanning process the geometric accuracy of the simulation mod-

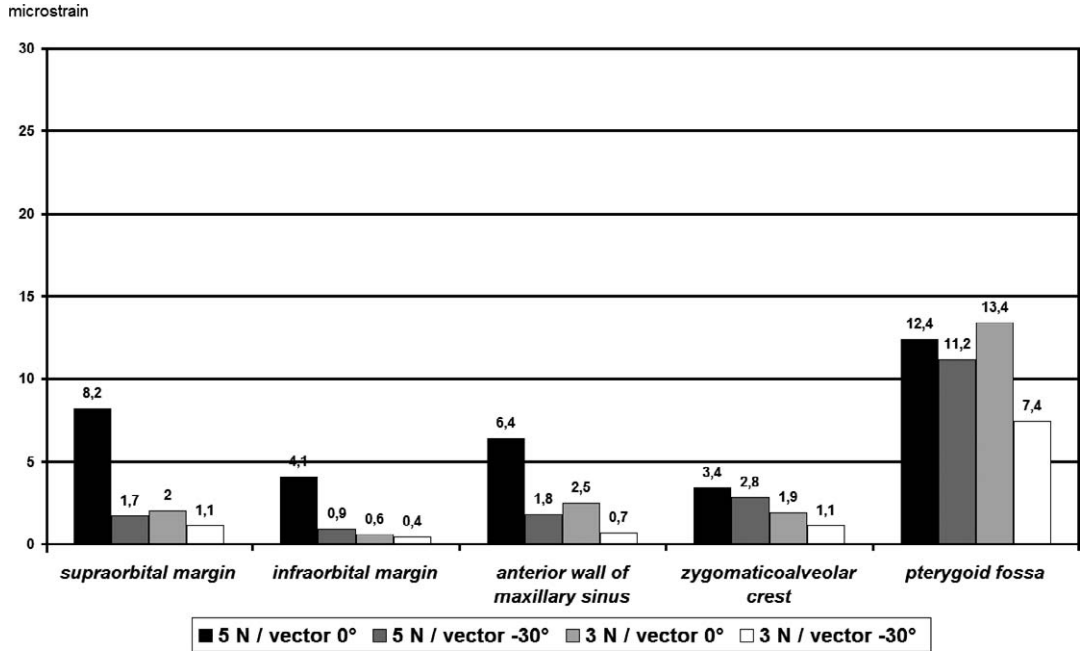

Figure 6. Strain values at the structures of the midface with horizontal pulling at 5 N and at 3 N in the anterior (vector 0°) and in the anterior caudal (vector −30°) direction.

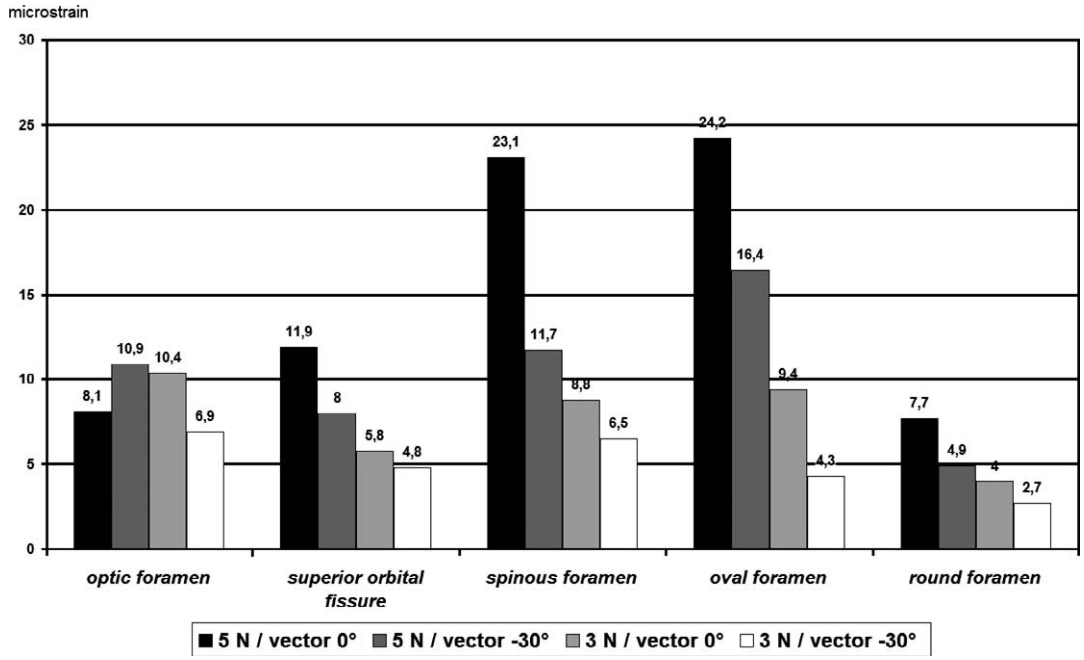

Figure 7. Strain values measured at the foramina of the cranial base with horizontal pulling at 5 N and at 3 N in the anterior (vector 0°) and in the anterior caudal (vector −30°) direction.

el was lower than that of the plastic skull. Nevertheless, the anatomic precision of the used FEM model was much higher than all skull models published so far. Certainly, the situation in individual patients can deviate from such averaged strain distributions. Also, a wide range of strain values was evident for each individual anatomic structure so that we only listed the maximum and minimum strains so as to ensure that the entire range of possible strains could be recorded for each anatomic structure.

Whereas other authors[22,24,25] measured the distribution of stress upon simulation of a maxillary protraction therapy, we measured strains in μstrain so that a comparison with Frost thresholds could be facilitat-

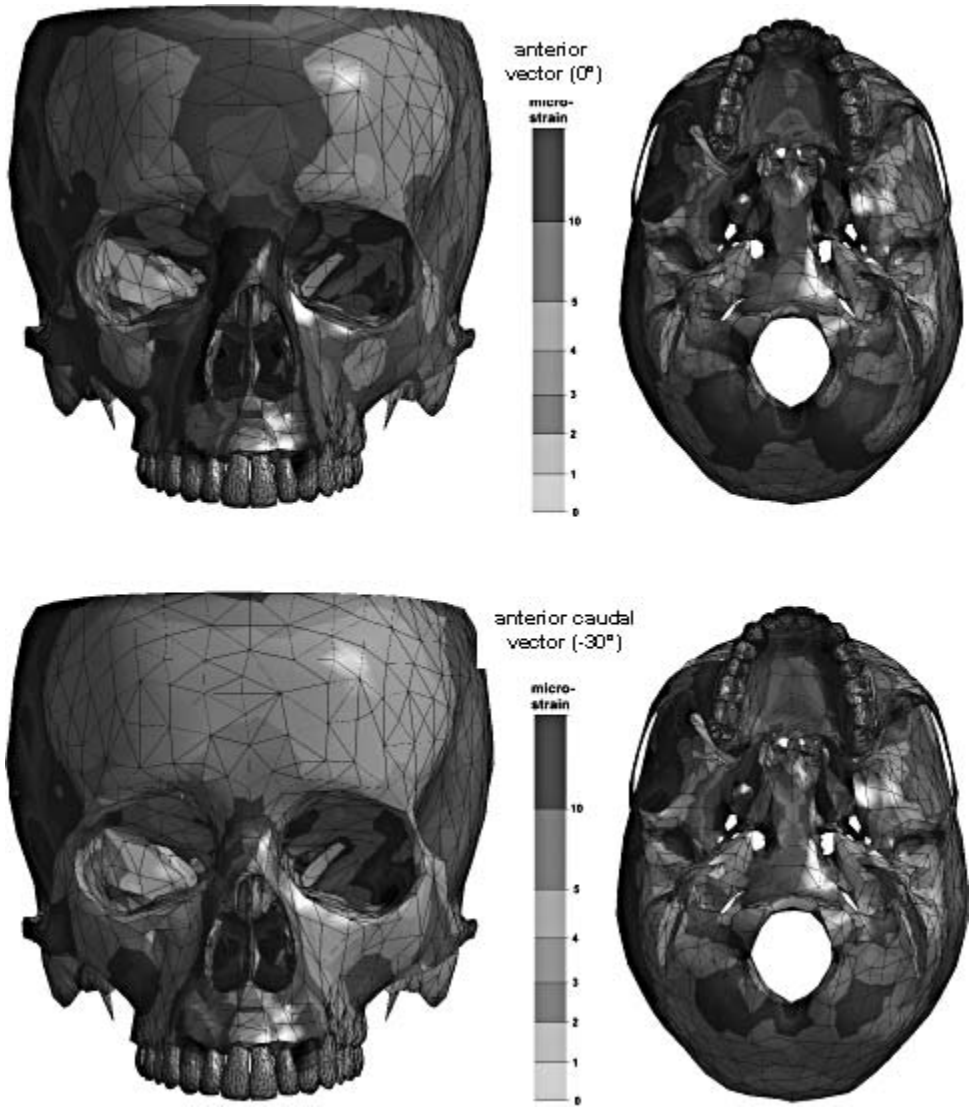

Figure 3. Distribution of the strains in the midface and at the cranial base when applying maxillary protraction with 2 × 5 N and an anterior (upper figures) and anterior caudal (lower figures) vector.

ed.[26–28] When comparing individual studies[22,24,25] with the results of the present study, an agreement with the distribution pattern of stresses in the midface was shown. With a purely anterior directed protraction of the maxilla with 5 N, excessively high strains in the area of the sutures of the nasal bone occurred, which were not observed when applying force anterior caudally or when applying smaller forces (3 N). If one looks at the level of the measured maximum strains, it can be seen that they were rather moderate. With a force application of 5 N the maximally measured strains in the midface lay at 26.4 μstrain and 24.2 μstrain at the cranial base. Usually, however, the maximum strains measured lay below 10 μstrain.

As Frost showed in 1983,[26] the skeletal effect of an applied force depends on the extent of strain achieved in the bone.[26–28] In order to achieve a growth-stimulating effect in the bone (remodeling), a strain of at least 2000 μstrain must be achieved (Frost's threshold). This value is not even approached in this study, with the measured strains being smaller by a factor of about 100. It should also not be forgotten that the Frost threshold applies for remodeling effects with nongrowing bone, and that it is unclear how high strains must be with growing bone to achieve a growth-stimulating effect.

Because of the large gap between the measured strains and the Frost thresholds, however, one is certainly entitled to doubt whether maxillary protraction therapy would have any significant effect on skeletal growth, particularly in situations where the sutures are already closed. This would confirm the results of Sung et al,[11] who could not confirm any skeletal effect of maxillary protraction therapy compared to an age-

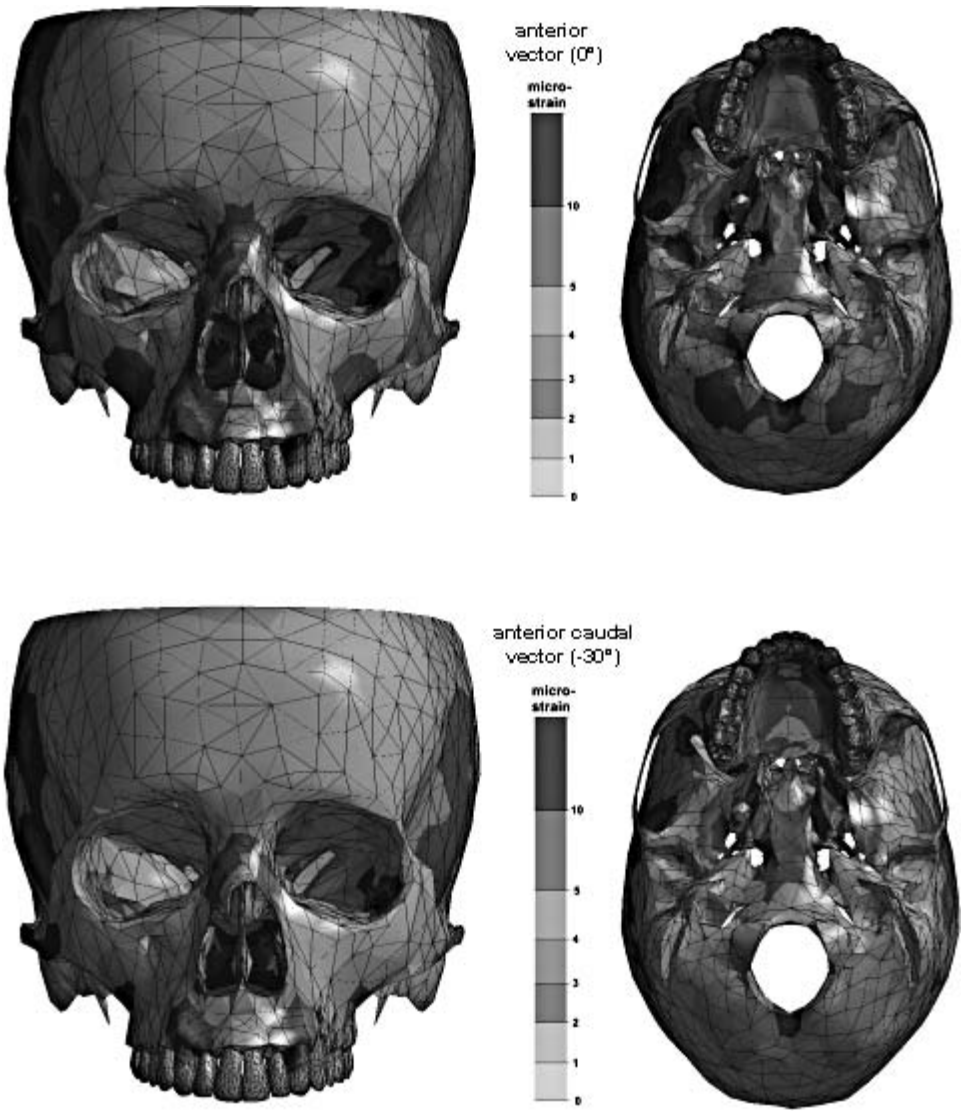

Figure 2. Distribution of the strains in the midface and at the cranial base when applying maxillary protraction with 2 × 3 N and an anterior (upper figures) and anterior caudal (lower figures) vector.

matched control group. Apparently, it cannot be excluded that the already demonstrated good clinical effectiveness of maxillary protraction therapy is based primarily on dental effects, while its skeletal effects remain a matter of some disagreement.)

CONCLUSIONS

- The strains occurring during a maxillary protraction therapy in the area of the midface and cranial base sutures are relatively small, a fact that renders a growth-stimulatory effect of the induced strains as rather improbable.
- Apparently, the good clinical effectiveness of the maxillary protraction therapy is based on dental effects, and not on a primarily skeletal efficacy of the dental equipment.

REFERENCES

1. Delaire J. The frontomaxillary suture. Theoretical bases and general principles of the application of postero-anterior extraoral forces to the orthopedic mask. *Rev Stomatol Chir Maxillofac.* 1976;77(7):921–930.
2. Delaire J. Maxillary development: therapeutic results. *Mondo Odontostomatol.* 1974;16(3):331–348.
3. Komposch G, Lux CJ, Stellzig-Eisenhauer A. Kieferorthopädische Wachstumsbeeinflussung. In: Diedrich P, ed. *Praxis der Zahnheilkunde, Kieferorthopädie II.* München, Jena: Urban & Fischer; 2000:47–66.
4. Jager A, Braumann B, Kim C, Wahner S. Skeletal and dental effects of maxillary protraction in patients with angle Class III malocclusion. A meta-analysis. *J Orofac Orthop.* 2001;62:275–284.
5. Delaire J. Maxillary development revisited: relevance to the orthopaedic treatment of Class III malocclusions. *Eur J Orthod.* 1997;19(3):289–311.

6. Delaire J. Manufacture of the ''orthopedic mask.'' *Rev Stomatol Chir Maxillofac.* 1971;72(5):579–582.
7. Hegmann M, Ruther A. The Grummons face mask as an early treatment modality within a Class III therapy concept. *J Orofac Orthop.* 2003;64(6):450–456.
8. Keles A, Tokmak EC, Erverdi N, Nanda R. Effect of varying the force direction on maxillary orthopedic protraction. *Angle Orthod.* 2002;72:387–396.
9. Hiyama S, Suda N, Ishii-Suzuki M, Tsuiki S, Ogawa M, Suzuki S, Kuroda T. Effects of maxillary protraction on craniofacial structures and upper-airway dimension. *Angle Orthod.* 2002;72:43–47.
10. Suda N, Ishii-Suzuki M, Hirose K, Hiyama S, Suzuki S, Kuroda T. Effective treatment plan for maxillary protraction: is the bone age useful to determine the treatment plan? *Am J Orthod Dentofacial Orthop.* 2000;118:55–62.
11. Sung SJ, Baik HS. Assessment of skeletal and dental changes by maxillary protraction. *Am J Orthod Dentofacial Orthop.* 1998;114:492–502.
12. Kim JH, Viana MA, Graber TM, Omerza FF, BeGole EA. The effectiveness of protraction face mask therapy: a meta-analysis. *Am J Orthod Dentofacial Orthop.* 1999;115:675–685.
13. Cha KS. Skeletal changes of maxillary protraction in patients exhibiting skeletal Class III malocclusion: a comparison of three skeletal maturation groups. *Angle Orthod.* 2003;73:26–35.
14. Merwin D, Ngan P, Hagg U, Yiu C, Wei SH. Timing for effective application of anteriorly directed orthopedic force to the maxilla. *Am J Orthod Dentofacial Orthop.* 1997;112:292–299.
15. Ten Cate AR, Freeman E, Dickinson JB. Sutural development: structure and its response to rapid expansion. *Am J Orthod.* 1977;71:622–636.
16. Holberg C. Method, Device and Computer Product for Making a 3D Finite Element Model. European Patent Office WIPO (PCT) 2003; Publication Number WO 03/10276.
17. Iseri H, Tekkaya AE, Oztan O, Bilgic S. Biomechanical effects of rapid maxillary expansion on the craniofacial skeleton, studied by the finite element method. *Eur J Orthod.* 1998;20:347–356.
18. Jafari A, Shetty K, Kumar M. Study of stress distribution and displacement of various craniofacial structures following application of transverse orthopedic forces—a three-dimensional FEM study. *Angle Orthod.* 2003;73:12–20.
19. Holberg C. Effects of rapid maxillary expansion on the skull base—an FEM-analysis. *J Orofac Orthop.* 2005;66:54–66.
20. Holberg C, Schwenzer K, Rudzki-Janson I. Three-dimensional soft tissue prediction using finite elements. Part I: Implementation of a new procedure. *J Orofac Orthop.* 2005;66:110–121.
21. Holberg C, Heine AK, Geis P, Schwenzer K, Rudzki-Janson I. Three-dimensional soft tissue prediction using finite elements. Part II: clinical application. *J Orofac Orthop.* 2005;66:122–134.
22. Miyasaka-Hiraga J, Tanne K, Nakamura S. Finite element analysis for stresses in the craniofacial sutures produced by maxillary protraction forces applied at the upper canines. *Br J Orthod.* 1994;21:343–348.
23. Verrue V, Dermaut L, Verhegghe B. Three-dimensional finite element modelling of a dog skull for the simulation of initial orthopedic displacements. *Eur J Orthod.* 2001;23:517–527.
24. Tanne K, Hiraga J, Kakiuchi K, Yamagata Y, Sakuda M. Biomechanical effect of anteriorly directed extraoral forces on the craniofacial complex: a study using the finite element method. *Am J Orthod Dentofacial Orthop.* 1989;95:200–207.
25. Tanne K, Hiraga J, Sakuda M. Effects of directions of maxillary protraction forces on biomechanical changes in craniofacial complex. *Eur J Orthod.* 1989;11:382–391.
26. Frost HM. A determinant of bone architecture: the minimum effective strain. *Clin Orthop.* 1983;175:286–292.
27. Frost HM. Skeletal structural adaptations to mechanical usage (SATMU): 1. Redefining Wollf's law: the bone remodelling problem. *Anat Rec.* 1990;226:403–413.
28. Frost HM. Skeletal structural adaptations to mechanical usage (SATMU): 2. Redefining Wollf's law: the bone remodeling problem. *Anat Rec.* 1990;226:414–421.